

The Solution Precursor Plasma Spray (SPPS) Process: A Review with Energy Considerations

Eric H. Jordan, Chen Jiang, and Maurice Gell

(Submitted February 12, 2015; in revised form June 27, 2015)

Solution precursor plasma spray (SPPS) is a coating deposition process that uses conventional plasma spray equipment, and solution precursors, rather than ceramic or metal powders, as starting materials. Because the process is exposed to oxygen at high temperatures, nearly all coatings, to date, are oxide ceramics. In this review, both the advantages and the disadvantages of the SPPS process and some comparisons made to the suspension plasma spray (SPS) process will be discussed. The advantages of the SPPS process include rapid exploration of compositions and fabrication of advanced coatings with unique microstructural features. Examples presented span densities from porous thermal barrier coatings (TBCs) to dense TiO₂ coatings. Two TBCs are in an advanced development stage: (1) a low thermal conductivity YSZ TBC and (2) a high-temperature yttrium aluminum garnet TBC. As for disadvantages, there are (1) the additional development work for each new precursor and (2) a lower standoff distance and deposition rate than the APS process, related to the evaporation of the solvent. The SPS process shares the same disadvantages. In developing new coatings, a number of factors should be considered and understood, which would help to shorten future development efforts. Future directions of the SPPS process will also be discussed.

Keywords deposition efficiency, heat transfer, microstructure, particle plasma interaction, solution precursor spraying, suspension spraying, thermal barrier coatings (TBCs)

1. Introduction

Solution precursor plasma spray (SPPS) is a variation of conventional plasma spray in that it uses the same plasma spray equipment. In conventional plasma spray, 10–100 μm, flowable powders of the final coating material are fed into the plasma, melted, and deposited as splats. In the SPPS process, an aqueous or non-aqueous solution containing the cation(s) necessary to form the oxide of interest is fed into the plasma to form the coating. Several previous reviews on the SPPS process have appeared (Ref 1–5) each with a different perspective and in this review, an additional perspective is presented. The steps in the SPPS process consist of droplet break-up, solvent evaporation, particle pyrolysis, melting, and finally deposition. The SPPS process, as illustrated in Fig. 1, shares much in common with the more widely studied suspension plasma spray (SPS) process (Ref 1, 2) where the coating material

is delivered into the plasma jet as suspended solid particles in a nanometer or micron size range. Both processes use similar liquid injection methods and share the challenge of the energy penalty needed to evaporate the suspending medium or the solvent. The most common injection method is direct injection of a solid stream of liquid. The high-velocity plasma jet causes cross jet atomization of the continuous cylindrical liquid stream. Alternatively, the suspension or solution can be atomized prior to contact with the plasma jet. In both processes the maximum equivalent loading of the coating materials is approximately 25% by weight (Ref 6), when normal liquid media are used. The maximum loading exists either because of the saturation limit of the precursor solution or suspension, or due to the increased viscosity that is difficult to overcome. The delivery of 25 wt.% feedstock in the SPPS and SPS processes, when compared to 100% in the atmospheric plasma spray (APS) process using powders, results in a significantly lower deposition rate.

An interesting exception to the equivalent oxide loading limit for the SPS process was recently developed, by overcoming the increased viscosity. This method uses a high viscosity liquid acrylic material as the suspending medium resulting in loadings as high as 50% by weight (Ref 7). The use of acrylic suspending media, however, creates a significant clean-up problem, and will not be further discussed here.

Both SPPS and SPS processes allow the creation of finer microstructures than the conventional powder spray, where the injection of powders finer than about 10 μm is difficult because the surface forces acting on the powder particles become dominant over the inertia forces leading

Eric H. Jordan, Department of Mechanical Engineering, University of Connecticut, Storrs Mansfield, CT; and Chen Jiang and Maurice Gell, Department of Materials Science and Engineering, University of Connecticut, Storrs Mansfield, CT. Contact e-mail: chenjiang.chn@gmail.com.

to powder agglomeration during feeding. In addition, much shorter standoff distances are usually required in both SPPS and SPS processes leading to manufacturing challenges, especially for complex geometry components.

The first attempts at the SPPS process were reported by Karthikeyan et al (Ref 8); however, powders rather than coatings were produced in that effort. The first coatings made were reported in Ref 9 and subsequently many additional coatings have been reported as well as process models. Limited selections of studies involving the development of the SPPS process include (Ref 3-5, 8-54). In the following few paragraphs some aspects of the SPS process are compared with the SPPS process, especially with respect to their similarities relating to thermal energy usage.

The SPS process requires a suitable way to suspend the materials of interest using either ionic or steric stabilization. Even powders of the same composition depending on surface properties may have different requirements for stabilization. Yet suspension stabilization is often more straightforward than choosing suitable chemical precursors for the SPPS process. In the SPPS process there are several complications, including finding a high molarity precursor for which the viscosity is low enough for injection, and dealing with the release of any gases generated from the decomposition stage, which is responsible for the low-density by-products in the cases of some precursors. Acquiring stable precursor solutions from soluble and mutually compatible chemicals in a given solvent is also challenging.

A unique feature of the SPPS process, which can be either an advantage or a disadvantage, is that chemical precursors can exhibit endothermic or exothermic chemical reactions, or a combination of both during pyrolysis, and the specific energy of these reactions is often sufficiently high so as to have an important effect on particle decomposition and melting. As such, the SPPS process requires considerable development effort for each new precursor composition. On the other hand, once a compatible chemistry is found, it is possible in a single spray session to explore many different compositional ratios, while for conventional spray this would usually take a much longer time because of the tedious powder synthesis procedures, which includes creating powder in sprayable forms, for example, by spray drying and sintering.

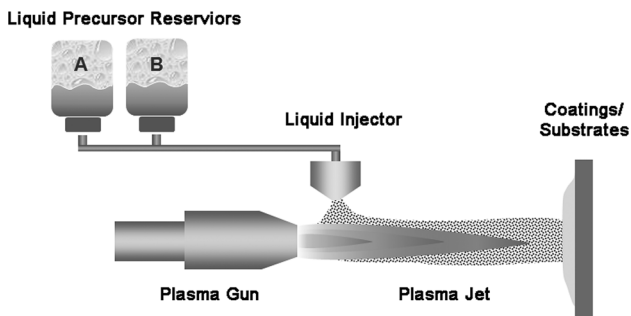


Fig. 1 Schematic illustration of the SPPS process

In light of the above, the disadvantage of both the SPS and SPPS processes with respect to the energy needed and the associated lower deposition rate will be presented. Following that is a discussion of general issues associated with the SPPS process including atomization and entrainment, the problem of small particle deposition, solution molarity, and endothermic and exothermic chemistry. Some strategies found useful in shortening the hunt for useful precursors are provided. Multiple examples of successful coatings will be presented to illustrate the exploitation of different unique aspects of the SPPS process, including rapid compositional exploration, exothermic reactions, unique microstructural features useful for thermal barrier coatings, creation of metastable phases, and the production of more homogeneous two-phase microstructures. In addition, we will include a brief discussion on the possibility of solution spraying using an HVOF torch.

2. Consideration of Energy Limitations: Powder Spray Compared to SPPS and SPS Processes

Thermal spray processes were performed with a Sulzer-Metco 9MB gun at UConn, and the results are compared between APS and SPPS of alumina. Relative deposition rates are examined for trials using typical parameters, based on our decade's long experience. It is then postulated that the difference in deposition rates between SPPS and APS processes is fundamentally dictated by the energy required to form melted ceramic. The values presented are not precise because of the wide variations in all possible spray practices, but are used to illustrate the important energy issues involved in these processes. As a starting point, the total power available after subtracting energy lost to the cooling water and lead wires is calculated from measured lab data. Table 1 shows the characteristics of the 9MB based on measuring the water temperature change, flow rate, and the voltage drop in the lead wire.

It is interesting to note that the grams/second for APS powder spray and solution spray are in the same range (Table 1). However, 4 times more ceramic is in fact injected into the plasma per second in the APS process, compared to the SPPS process (or similarly the SPS process). This ratio is based on an assumed 20% of oxide by weight in both SPS suspensions and SPPS precursor

Table 1 Measured characteristics of the Sulzer-Metco 9MB plasma gun

Electrical power at the power supply	70 V, 500 A, 35 kW
Electrical power at the gun	65 V, 500 A, 32.5 kW
Temperature change based lost power	14.6 kW
Net energy in the plasma jet	21 kW
Typical powder flow rate of Al ₂ O ₃	0.63 g/s (5 lbs/h)
Typical precursor flow rate, density ~1.3 g/mL	0.76 g/s (35 mL/min)

solutions. If similar deposition efficiency for all three processes is assumed, the deposition rate ratio would also be 4:1. The lower oxide feeding rate, then, appears to be the primary factor leading to lower deposition rates in the SPPS and SPS processes compared to the APS process.

Generally speaking, in the SPPS process the liquid precursor in the plasma jet goes through a series of steps, as have been described in some modeling papers (Ref 26, 30, 50, 51). Following the atomization either in an atomizing nozzle or by the force of the plasma jet, the droplet quickly reaches the approximate velocity of the surrounding jet (Ref 55). The solvent then starts to evaporate. The modeling results show that the heat transfer within the droplet is so rapid that it remains essentially isothermal. Evaporation is typically fast compared to diffusional mixing, and there is a tendency for the solute to become concentrated near the surface (Ref 50, 51). In areas where the solvent has evaporated there are a series of events that may include, driving off the hydrated water (for nitrates), pyrolysis of the precursor, heating of the oxide, and then final melting. As a result, the major steps to be completed from an energetic point of view are (1) solvent evaporation, (2) turning the precursor into an oxide (pyrolysis and in some cases loss of hydrated water), (3) heating the oxide to the melting temperature, and (4) oxide melting.

The power required to melt the ceramic during continuous feeding is therefore calculated at the feed rates from Table 1, as follows:

- For standard APS process using powders: heat the powder (alumina) to the melting point, and then melt the powder;
- For the SPPS process: heat the precursor to boiling point, boil all the solvent, heat the particles to the melting point, and then melt the oxide.

It is worth noting here that specific heat is a function of temperature, and when calculating the enthalpies over a large temperature range, the effect of changing specific heat should not be ignored. Therefore, empirical formulae of specific heat are used in this calculation, and the resulting energy consumptions for both APS and SPPS processes are shown in Table 2.

Remarkably, the power utilized is nearly the same in both powder and solution spraying, and that amount of power (Table 2) is approximately 10% of the available power in the plasma jet (Table 1). This result is consistent

Table 2 The comparison of energy consumption between APS and SPPS processes

System	Air plasma spray	Solution precursor plasma spray
Heat liquid or solid to 100 °C, kW	1.595	0.210
Heat of vaporization ^a , kW		1.345
Heat to melting point, kW		0.403
Heat of fusion, kW	0.688	0.178
Total power, kW	2.283	2.137

^aNot present in the case of APS

with the hypothesis that both APS and SPPS deposition rates are limited by the amount of heat that can be transferred to the material, and this available transferable heat is nearly the same for both APS and SPPS processes. The higher deposition rate in the APS process is due to the much lower energy requirement of converting a unit amount of ceramic powders to the final melted materials, compared to producing melted ceramics from liquid precursors in the case of solution spraying. For a more direct visual comparison, Fig. 2 is provided showing the different energy amounts needed for each of the transformation steps in the SPPS process listed in Table 2.

It is clear that the greatest fraction of energy in the SPPS and the same as for the SPS processes is used to evaporate the solvent or the suspending medium. Accordingly, it may be helpful to use a liquid with a low heat of vaporization that is compatible with the process, to minimize the energy penalties lost to the evaporation of dispersing media. Table 3 compares the heat of vaporization of some possible polar solvents, indicating that there is a potential for increased material deposition rates if such solvents are utilized.

In addition, organic solvent could provide extra energy when it burns, and this in moderation can be useful in our experience. However, it should be noted that recent results have indicated the heat of combustion, for example from using ethanol, is manifested sufficiently far downstream in the plasma jet to be of little value for heating the delivered materials (Ref 53), in cases where the melting

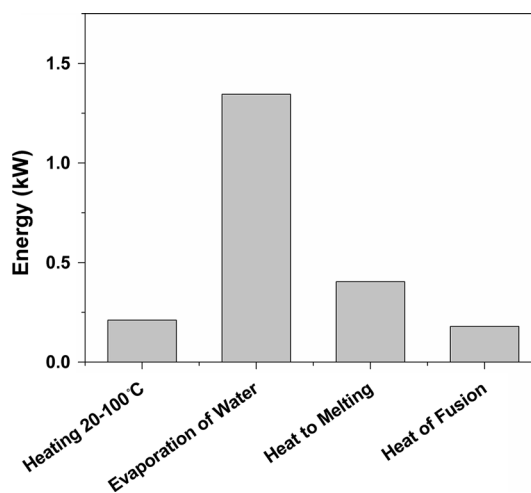


Fig. 2 Energy used in each step of forming molten ceramic starting with a water-based liquid precursor

Table 3 Heat of vaporization of some polar solvents used in the SPPS process

Solvent	Heat of vaporization, kJ/g
Water	2.26
Ethanol	0.841
Ethyl acetate	0.3625

point of the material is higher than the expected temperature from burning the organic solvent. The heat from the combustion of the organic solvent can potentially cause the substrate overheating; however, this heating can be remedied by modified processing conditions, such as faster scan speeds or in-process cooling particularly with parts on a rotating table. In the end, the benefit of using organic solvents is another example of a factor that can be either useful or harmful depending on the specific situation.

In summary, it appears that the primary cause of the observed lower deposition rate for the SPS and SPPS processes is the energy penalty associated with the need to evaporate solvent or suspending medium, which accounts for more than 50% energy loss. Using solvents with lower heat of vaporization can potentially improve deposition rates. As will be discussed for the SPPS process, chemical reactions with energy release involving an oxidizer that is part of the chosen precursor for example nitrates may increase deposition rates by introducing heat. Oxygen that is part of the precursor is fundamentally different from that coming from the ambient air, as it affects the precursor pyrolysis behavior in the presence of the inert primary gasses (argon, nitrogen, or helium) and the reducing secondary gas (hydrogen). As a result, the entrainment of atmospheric oxygen is essential for the combustion of the organic solvent, with the absence of any oxidizer as part of the precursor. Based on the measurements, the combustion appears to happen significantly downstream of the injection location (Ref 53). At this location the coating materials are hotter than upstream, making heat transfer to the coating materials less effective. In addition, as the available oxygen occurs downstream there is less time for the beneficial heat transfer to occur. In our experience, with greater amounts of organic solvents, the downstream burning of the organic solvent is possibly responsible for the substrate overheating issues. On the other hand, the experience with exothermic precursors is that relatively denser coatings are produced, due to better in-flight heating and melting. However, too much exothermic energy can also cause problems.

3. Basic Issues in the Solution Plasma Spray Process

3.1 Particle Size

In the SPPS process, very fine particles can be produced depending on the solution concentration and the size of the resultant droplets. Typically, the materials deposited in the SPPS process range from 0.5 to 4 μm in diameter, based on the observed deposited splat structure (Ref 10). But it is possible that the particles present can be even finer than that. If an arriving particle is too small it will follow the gas stream as it bends to go around the substrate. The result will either be that the particles are not deposited or that they can arrive at a low incident angle producing cauliflower or feathery features, subject to the shadowing effect. This particle behavior is governed

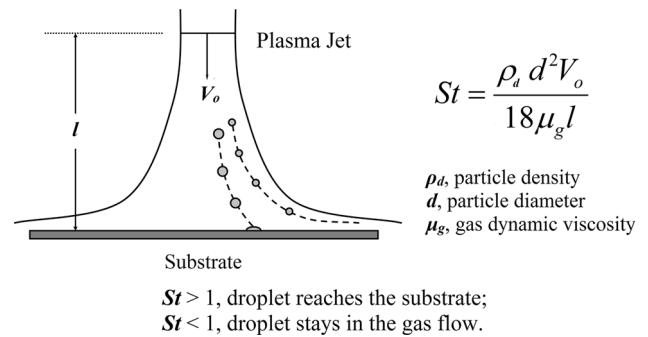


Fig. 3 Stokes number for in-flight particles and the effect on deposition

by the Stokes number as illustrated in Fig. 3, where Stokes numbers less than one are generally associated with particles following the gas stream. For the bond-coated or grit blasted surfaces that are used in the SPPS process, the roughness is typically measured as $Ra = 3\text{--}5 \mu\text{m}$. Much rougher surfaces when exposed to small particles following the gas path nearly parallel to the free surfaces would be expected to suffer more apparent shadowing effect that in most cases produces porous-branched structures that are friable and not suited for most purposes. As a result, processing conditions are normally adjusted to avoid such structures. In suspension spray though, careful orchestration of this particle behavior as well as surface roughness was demonstrated (Ref 56) to produce the stress-relieving columnar structures in desirable thermal barrier coatings to accommodate the thermal expansion mismatch between the coating and substrate, while similar microstructures can also be replicated with the SPPS process.

It is, therefore, necessary to manage particle size distributions when using either the SPS or SPPS process so as to obtain desired microstructures. Particle size control is difficult and indirect though in the SPPS process, because the droplet size will not usually determine the particle size of arriving materials due to the occurrence of droplet break-ups in the plasma jet. Complete characterization of the droplet sizes generated is possible (Ref 55); however, mass balance and experimental observations of coating and splats (Ref 10) indicate that in the SPPS process droplet break-up is more of the rule than of the exception. In addition, because of the absence of effective diagnostic instrument for these small droplets, much of the trial and error in developing the SPPS process is then connected with using empirical relationships between process variables and the arriving particle size. Typically, denser structures require large particles and hence larger droplets arriving more normal to the surface, and shadow-based cauliflower structures require oblique incident material that is expected for smaller arriving particles and hence smaller droplets. Understanding such trends is useful in the process development for SPPS and SPS coatings. But again, the control of this is still a challenge because of the indirect relationship between droplet sizes and particle sizes arriving at the substrate created by droplet break-up.

3.2 Droplet Injection Pattern Geometry Entering the Plasma

The plasma jet exiting the gun has a strong variation in temperature and velocity, both radially within a given plane of the plasma plume and axially. Consequently, the path that an injected particle takes in the plasma plume and its associated heating is strongly affected by where it is injected into the jet, as shown in simulations (Ref 25). Materials on trajectories that are in the cooler, slower regions of the jet generally are associated with lower density coatings and lower deposition efficiency. To inject the bulk of the materials into the part of the plasma with high deposition efficiency, it is desirable to have the projected area of the liquid jet on the plasma plume boundary as small as possible. At the same time, it is desirable to have as uniform a droplet size distribution as possible to avoid low deposition efficiency or cauliflower/feathery microstructures due to small droplets with low Stokes number and partially pyrolyzed or even unpyrolyzed materials being deposited due to very large droplets. Figure 4 shows a summary of an experiment in which a pressure atomizing nozzle with a pressure fan pattern of 15° divergence fed with a bubbly liquid (evanescent atomization) was brought increasingly close to the plasma plume periphery. This progressively reduces the size of projected areas on the plasma plume and associated variation in droplet trajectories in the jet. As can be seen, as the projected area gets smaller, the coating hardness increases while the porosity decreases. Additionally, not shown in the figure is that the deposition efficiency also increased by over a factor of 2 as the injector was brought closer to the plasma plume. To inject the bulk of the materials into the part of the plasma with high deposition efficiency, it is desirable to have the region into which the droplets are injected into the plasma as small as possible.

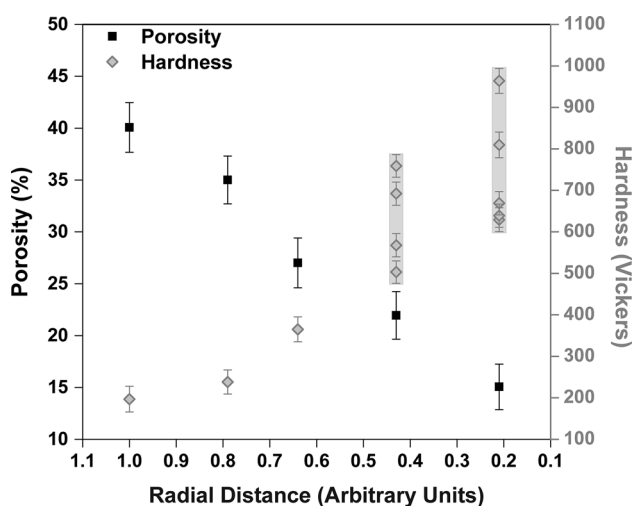


Fig. 4 The coating porosity and hardness varied with the particle injection footprint. Note: the smaller injection projected area also made coating microstructure sensitive to particle entrainment, rendering wider hardness distributions

3.3 Precursor Molarity

Because of the limits on how much liquid can be processed using liquid injection (SPPS or SPS), it is economically desirable to increase deposition rate by increasing the molarity of the precursor solution/suspension. This can be done only up to a limit, because of the solubility limits and the increased precursor viscosity. When the molarity is increased, the coating density increases as shown in Fig. 5 (Ref 31). The range of equivalent end products solids loading that is acceptable to the process varies from 1 to 30% by oxide weight. Solutions should not be used too close to the solute solubility limit because precipitation can occur and cause clogging issues in the delivery system, due to small fluctuations in temperatures; therefore, solutions are generally used at 80% or less than the absolute solubility limit in our regular spray trials, when the maximum solution viscosity viable in our equipment is 15cP. Processing of higher viscosity liquids may be possible using higher pressure at delivery. Besides, the use of more powerful plasma guns allows higher flow rates at the liquid injectors based on energy limitations. Consequently, larger diameter injectors will have lower pressure drop for a given viscosity, and would be more difficult to clog.

3.4 Precursor Energetics

In the SPS process, the primary exothermic event expected is in the burning of organic suspending agents,

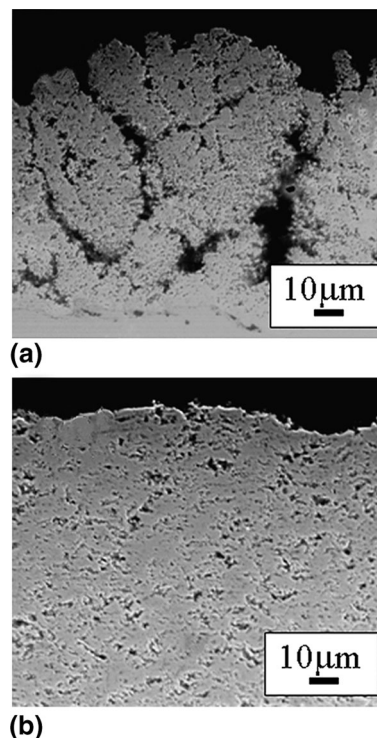


Fig. 5 Cross section micrographs of YSZ coatings made from precursor solution with (a) low molarity and (b) high molarity

Table 4 Fluid and thermal properties of various Y₂O₃/MgO precursor solutions compared with those of YSZ (Ref 20)

Precursor type	Viscosity, mPa·s	Surface tension, mN/m	Exothermic heat, J/g	Endothermic heat, J/g	Net heat, J/g
Y[n]Mg[n]	2.26	46.51	0	−472.2	−472.2
Y[a]Mg[a]	1.24	48.54	0	−477.1	−477.1
Y[n]Mg[a]	1.43	66.40	722.0	−191.1	530.9
Y[n]Mg[n] + NH ₄ [a]	2.30	50.34	402.0	−175.5	226.5
YSZ	6.16	52.65	419.1	−33.4	385.7

Heat heat of decomposition reaction, *n* nitrate, *a* acetate

most frequently ethanol. Unfortunately the primary plasma gases are either inert (Ar, N₂ or He) or reducing (H₂). Accordingly, the heat released by oxidation of organic ingredients is delayed following injection until the plasma jet entrains sufficient oxygen to allow burning. As mentioned earlier, burning downstream (Ref 53) may overheat the substrate and not contribute much to processing the powders.

In the case of SPPS, it is possible to use precursors that contain both oxidizing and reducing agents in the same precursor. For example, acetate/nitrate combinations are typically employed for the deposition of YSZ TBCs (Ref 24). In addition to acetate combined with nitrates, controlled amounts of urea and/or ammonium acetate are also added occasionally as a fuel to react with the nitrates (oxidizers) (Ref 20). Table 4 shows the exothermic and endothermic events measured by differential scanning calorimetry (DSC) (Ref 20) for precursors with varying reducer/oxidizer ratios. Note that the energy for these events can be as large as 531 J/g, while the heat of evaporation of ethanol is just 841 J/g, which means the chemical energy is potentially significant, particularly because it is released next to the material to be deposited, avoiding issues related to heat transfer during short droplet flight times that occur for energy released from burning the solvent.

3.5 Precursor Screening

There is great complexity in the behavior of precursors in the SPPS process, with reaction-induced gas release being a concern. Depending on the physical properties of the precursor, gas release can lead to foaming and low-density deposits. In addition, modeling has clearly shown that solvent evaporation is very rapid compared to diffusional mixing leading to solute concentration in the outer part of the droplet (Ref 26). Furthermore, if the concentrated outer layer is gas impermeable, the evaporation of the inner liquid core can lead to the production of many sub-droplets by vapor driven explosions. The solute can go through a series of physical states: from the solution state, to a dried gel, to a molten salt, to several stages of reaction to form the final material. In light of this complexity and the lack of detailed properties of the intermediate states, accurate prediction of precursor behavior and suitability for a given process is currently not possible.

It is desirable to have a laboratory process for screening precursors, rather than having to conduct expensive plasma spray trials for each composition. Though the kinetics of precursor reactions will differ in a laboratory furnace and in the plasma, work over the years has demonstrated these screening tools can save considerable resources, before the final, confirmatory test concerning the plasma spraying. Experimental methods for screening precursors were described in Ref 20 and are to be summarized here.

For each new precursor considered, there are basic issues to consider with respect to acceptability. First, it is imperative that the precursor does not present an explosion hazard, as can be the case in highly reactive oxidizer-reducer combinations, especially if they are too close to the ideal stoichiometry. This danger is generally greater if non-aqueous solvents are used. Cation loading is another concern. Some precursors are too dilute to be useful, but this depends strongly on the materials and microstructural goals.

Secondly, each candidate precursor should be analyzed with differential scanning calorimetry (DSC) and thermogravimetry (TGA) to measure thermal characteristics. Large endothermic events will predict challenges in producing fully pyrolyzed materials. Exothermic peaks can aid material pyrolysis, but excessive exothermic energy can also cause deposition issues, including the production of very small droplets by violent reactions. Very small particles do not deposit efficiently, as determined by the small Stokes number. As a matter of routine, a small amount of each candidate precursor is also heated on a hot plate and the physical states the precursor goes through are observed. The formation of durable foams is a negative indication as to the future success of the precursor.

Finally, a useful screening method is to let the precursor fully react in a beaker and examine the by-products (Ref 20). In this procedure, all the solvent is evaporated in a low-temperature oven, and the dried gel is then heated in a muffle furnace with the temperature set above the pyrolysis temperature that is measured by DSC. Figure 6 shows the byproduct comparison of a precursor for making Y₂O₃-MgO composites that produced low-density coatings and one that produced dense coatings with high deposition efficiency. Note that the SEM photos of the respective furnace pyrolysis products show the one appearing to have low density is actually consisting of very porous particles while for the denser product the individual particles are dense. Considering the Stokes number

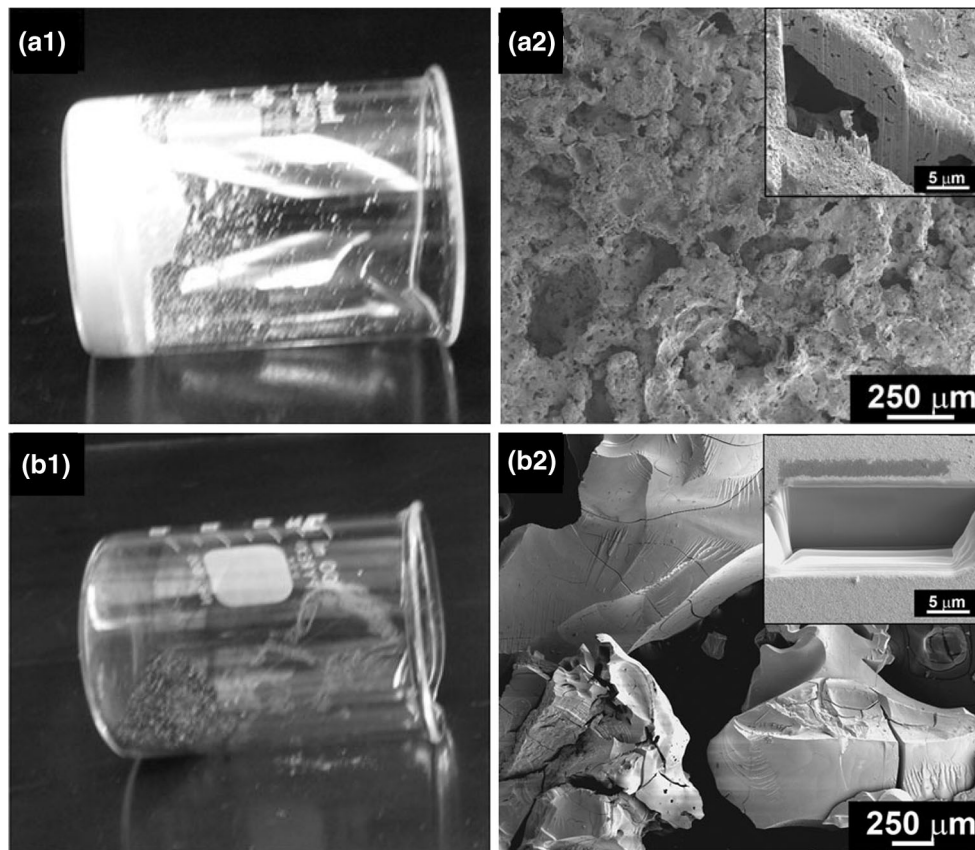
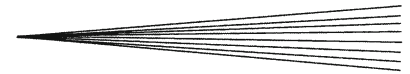


Fig. 6 Furnace pyrolysis test used for screening precursor compositions

effect of Fig. 3, denser particles are more likely to deposit down to smaller sizes and arrive at a higher velocity more normal to the surface, all of which leads to denser coatings compared to the porous particles. It is also expected that some of the porosity in the arriving particle will remain in the final deposit (Ref 57). The hot time in thermal spray is very short and porosity is not likely to disappear during such a short time. This is consistent with the observation that fused and crushed APS powder generally leads to denser coatings compared to porous coatings generally made from hollow HOSP spray powders (Ref 58). Though these presumptive arguments are not direct proofs showing low-density byproduct in the breaker will necessarily lead to low dense coatings, in the end this simple furnace pyrolysis test to date has proven to be very useful in screening potential precursors in our spraying practices (Ref 20).

In summary, pre-deposition precursor characterizations are recommended for successful depositions of new coating compositions, which include thermal characteristic screening with DSC, viscosity measurement, observation of the sequence of physical states upon slow heating on a small amount of precursor, and the examination of the nature of the materials created by rapid pyrolysis in a furnace. This screening will not guarantee that particular precursor is going to produce a viable coating but can with reasonable reliability eliminate further work on unpromising precursors.

4. Applications Demonstrating Unique, Useful Features of the SPPS Process

4.1 Thermographic Phosphors: Demonstrating Rapid Composition Exploration

A useful method of temperature measurement can be based on thermographic phosphors where a fluorescing coating is applied that has the property that over a specific range of temperatures, the decay time of the fluorescence changes exponentially with temperature, typically changing 2 to 3 orders of magnitude over a temperature range of 200-400 °C (Ref 34, 37). By measuring the decay time, accurate temperature measurements can be made. For very high temperatures, lanthanides are the widely used dopants. UConn was tasked with creating optimal high-temperature phosphor coatings based on Dy- and Tm-doped yttrium aluminum garnet (YAG, $Y_3Al_5O_{12}$). Generally, there is an optimal dopant level yielding maximum brightness while still preserving the ideal response which is disrupted at too high a concentration. Using the SPPS process it was then possible to produce both Dy- and Tm-doped YAG coatings with 0.5, 1, 3, and 5% for both dopants in a single day. To spray such coatings using powders on the other hand requires synthesizing different doped YAG powders ahead of time, and preparing the sprayable forms of these powders using spray drying and

heat treatment. This is rather time consuming and costly, as spray drying is largely a trial-and-error process and can easily consume months of effort. The SPPS Dy:YAG coatings were proven very successful and continued to allow temperature measurement even after the turbine blade to which it was applied was accidentally melted (Fig. 7).

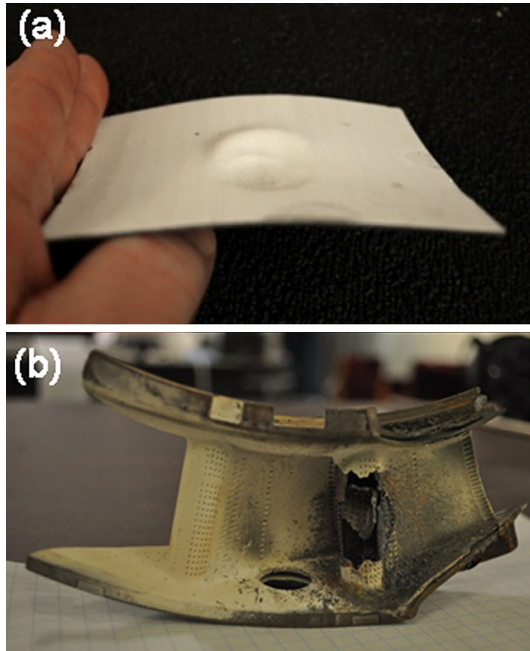


Fig. 7 SPPS Dy:YAG phosphor coatings survived and continued working after the underlying alloy melted due to ultra-high temperature

An effort to develop YAG as a promising topcoat material for thermal barrier coatings will be described subsequently. The sprayable powder of YAG was not commercially available, so the ease of exploring new compositions using the SPPS process was also of critical importance for the development of this new TBC topcoat material.

4.2 Dense Homogeneous Two-Phase Coatings Using the SPPS Process

It has been repeatedly shown that when mixed powders are used in the SPS and powder spray processes; there is a strong tendency for the two materials to exhibit phase separation during thermal spray (Ref 59, 60), leading to a coarse, two-phase microstructure. In SPPS, the material originates as a molecularly mixed solution. Figure 8 shows two alumina-doped zirconia coatings one using pre-mixed commercial powders and the other using the SPPS process (Ref 29). As can be easily seen, the SPPS coating is far more homogeneous. In addition, Fig. 8 indicates that high density coatings can also be produced using SPPS process in specific cases. In this particular case, in addition to choosing spray parameters expected to produce denser coatings, the precursor used was zirconia acetate with aluminum nitrate which is exothermic and leads to more complete melting and denser coatings. High density is also more common in relatively low melting point materials like TiO_2 . There is a repeated trend with respect to the spray parameters though that smaller standoff distances and lower precursor feed rates lead to density increases in the as-deposited coatings due to hotter substrate temperature and enhanced heat transfer, but the reason for getting especially dense coatings based on these trends for some materials but not others remains unclear.

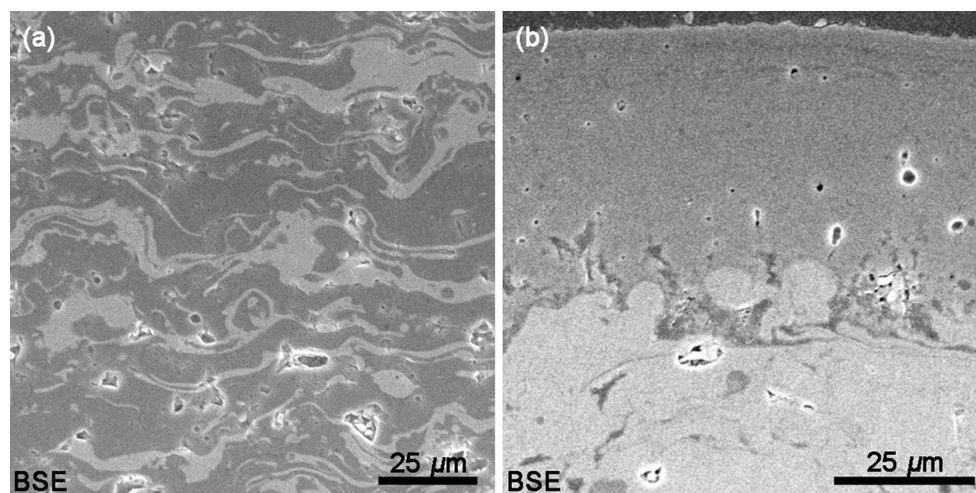


Fig. 8 (b) SPPS alumina-doped zirconia coatings made show increased homogeneity and density compared to those sprayed with (a) the traditional powder process

4.3 Unique Microstructural Features in SPPS TBCs

Thermal barrier coatings (TBCs) are applied in gas turbines to insulate the underlying metallic component from high temperatures, thus allowing the engines to operate at higher firing temperatures and achieve higher efficiency. The uses of SPPS process for producing TBCs were previously reviewed in (Ref 3, 4, 9). Thermal barrier coatings in gas turbines are subject to repeated straining each time the engine is turned on or off due to the difference in thermal expansion coefficient between the metal substrate and the ceramic topcoats. A well-recognized strategy for dealing with this mismatch strain is to create coating microstructures with through-thickness cracks that accommodate the thermal strains. This strategy is part of the reason for electron beam physical vapor deposited coatings (EBPVD) (Ref 61) and for dense vertically cracked coatings (DVCs) (Ref 62) both exhibiting extended service in aviation turbines. In the production of DVC coatings, the cracks are created by thermal shock and can only be created in relatively dense coatings (Ref 62). The SPPS process, on the other hand, can also create structures similar to DVC coatings, however by a different means. These stress-relieving through-thickness cracks in SPPS coatings appear as the deposited semi-pyrolized materials shrink due to further in-process heating (Fig. 9b) (Ref 17) and are not limited to only

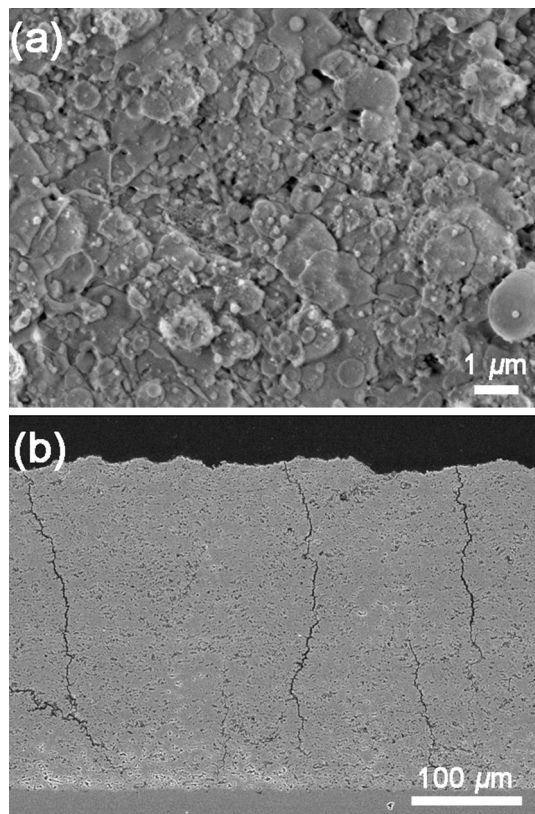


Fig. 9 Microstructural features of the SPPS TBCs: (a) small splat size, and (b) stress-relieving through-thickness vertical cracks

dense coatings. Thus, the SPPS process can produce through-thickness cracks and enhance durability to wider range of coating microstructures.

The easily reproducible stress-relieving cracks in the SPPS process offer the opportunity to use coating materials that otherwise might not be considered due to having a relatively large thermal expansion mismatch to the turbine alloys. Recently, this concept has been explored with respect to the TBC candidate material of yttrium aluminum garnet (YAG). This material has several attractive properties including lower density, phase stability up to the melting point, and high hardness for potentially good erosion performance. Novel YAG coatings have recently been made using the SPPS process and subsequent testing has shown that the coatings have cyclic furnace durability equal to or better than standard air plasma-sprayed YSZ, superior erosion performance, better high temperature stability, and sintering resistance (Ref 27). The through-thickness cracks made by the SPPS process along with the ability to spray new compositions without the difficult task of creating sprayable powder opens the door to exploring YAG and possibly other materials with less well-matched coefficients of thermal expansion compared to the substrate that have otherwise not been selected for extensive study. Another place where the through-thickness vertical cracks are found useful is in making very thick thermal barrier coatings. The cyclic durability of APS coatings decreases with increasing thickness with build-up of residual stresses. Thick SPPS vertically cracked coatings showed no such deficit (Ref 18) because of their strain-tolerant microstructure.

A second unique feature of the SPPS process is the fact that the splat diameters are on the order of 1-5 μm more than 10 times smaller than typical powder-sprayed splats (Fig. 9a). These finer structures have five times higher in-plane fracture toughness than conventional coatings as shown by indentation toughness testing (Ref 18). This higher toughness is partially responsible for the better than expected erosion performance of such coatings.

The third feature that can be produced by choice in the SPPS process is planer arrays of porosity which have been referred to as inter-pass boundaries (IPBs). In the correct processing window, that is primarily defined by a small offset between spray passes, IPBs can be repeatedly produced, which reduce the thermal conductivity and increase the thermal protection of the coating (Ref 23, 24). Recent efforts to minimize the thermal conductivity by producing optimal IPBs have resulted in a thermal conductivity as low as 0.63 W/mK in the YSZ TBCs, approximately half of the thermal conductivity made by the conventional methods (Fig. 10) (Ref 24), while corresponding cyclic furnace durability and erosion resistance were shown comparable to standard powder-sprayed coatings.

Finally, it is important to note that due to the small splat sizes associated with the SPPS process, the as-coated surface of SPPS TBCs are much smoother ($R_a=3\text{-}4\mu\text{m}^*$)

*All roughness data were measured from as-deposited TBCs or as-received samples, using the Phase II SRG-4500 Surface Roughness Profilometer.

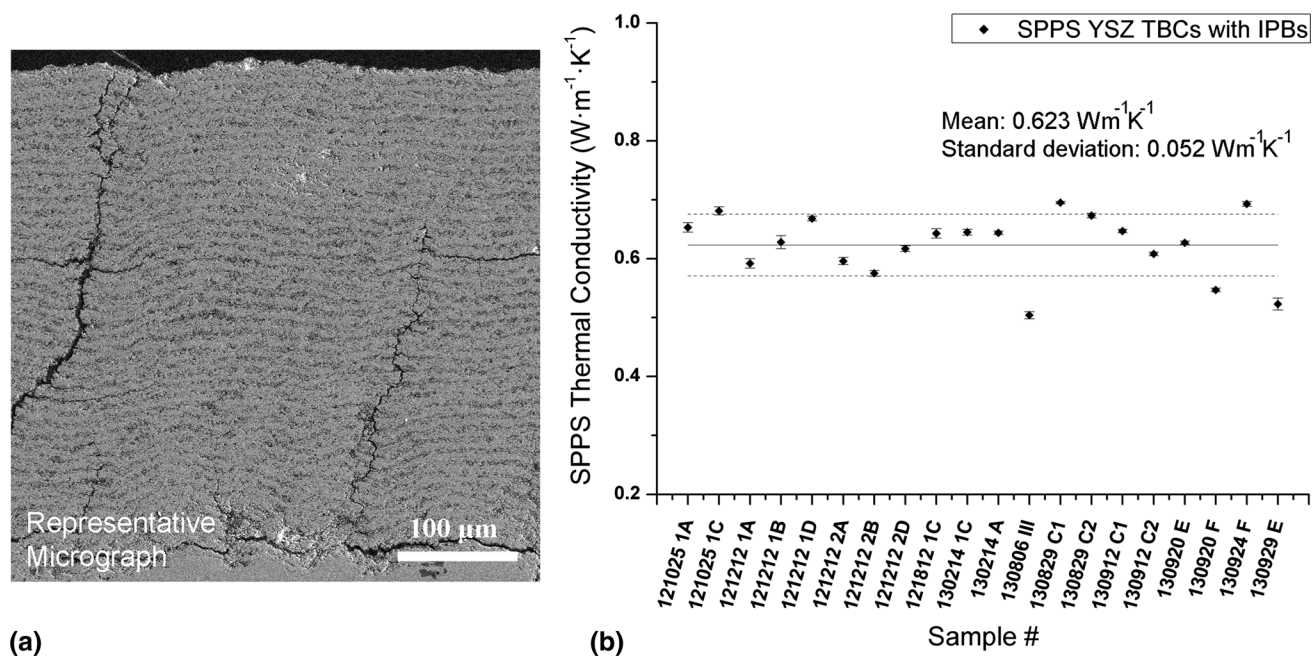


Fig. 10 Unique microstructural feature of inter-pass boundaries (IPBs) in SPPS TBCs can reduce coating's thermal conductivity by 50% (Ref 24)

than APS TBC ($Ra=9-10\ \mu\text{m}$) and approach the low surface roughness of EB-PVD TBCs ($Ra=2-3\ \mu\text{m}$), which provides additional aerodynamic and heat transfer benefits.

4.4 Metastable CMAS-Resistant TBCs Using SPPS

In the SPPS process, molecularly mixed solutions are melted and solidified very rapidly and as a consequence, metastable phases can be obtained, because there may not be sufficient time for equilibrium phases to form. This can either be a problem or an opportunity. In one instance, to make a thermal barrier coating that is more resistant to molten contaminants common in gas turbines, mainly of calcium-magnesium-aluminosilicate (CMAS) (Ref 22), excess alumina was found to have a beneficial reaction with CMAS, inhibiting its penetration into the TBC and mitigating the damage. Unfortunately, the equilibrium solubility of alumina in yttria-stabilized zirconia TBC is small. It was found that using the SPPS process up to 20% alumina could be held in the metastable solution of YSZ and this dramatically improved the CMAS resistance of the coating (Ref 22). Subsequently, this same coating was made by the conventional plasma spray process (Ref 63). The SPPS process with the advantage of rapid composition exploration was crucial in the discovery process and motivated the further development for the APS process.

4.5 TiO_2 Coatings Using SPPS

Dense coatings can be fabricated by the SPPS process. This is promoted by (1) using near saturation concentrations of the precursors (Ref 31), (2) full melting of the

precipitated materials, and (3) dense particle production from precursor droplets, and (4) other factors (Ref 20). In the experiments described in (Ref 21) a 1.5M solution of titanium isopropoxide in an ethanol solution was used, which is 50% of the 3M saturation concentration. TiO_2 has a relatively low melting point of 1840 °C, which helps in making a dense coating in that the arriving material was well-melted. The coating was sprayed using a Metco 9MB gun and the resulting coating was pure rutile (Fig. 11). By way of contrast, porous TiO_2 coatings have also been made by the SPPS process (Ref 33). These coatings were subsequently surface activated using a solution of KOH and the resulting coatings showed excellent ability to form hydroxyl apatite in simulated body fluids (Ref 32) indicating a potential for use in orthopedic implants.

4.6 Fuel Cell Applications

At least two interesting fuel cell applications have been made with the SPPS process. In one study $\text{La}_{1-x}\text{Sr}_x\text{MnO}_3$ was made by the SPPS process and the troublesome sub-oxides found in conventional APS deposition did not occur (Ref 40). This shows that the thermal history is sufficiently different between the SPPS and the APS processes, which yielded a unique and useful result. In a second study, a Ni-doped YSZ anode was successfully produced by hydrogen annealing the nickel oxide in the SPPS ceramic coatings back to nickel metal (Ref 19).

4.7 Coatings by HVOF SPPS Process

HVOF has been adapted successfully for suspensions as the liquid feedstock in a coating deposition process, known as high-velocity suspension flame spray (HVSFS).

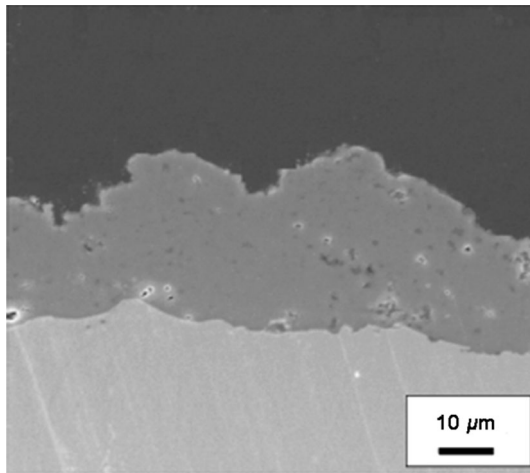
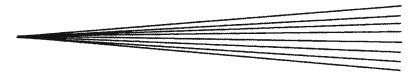


Fig. 11 Dense TiO₂ coatings produced by the SPPS process (Ref 21)

The considerations with respect to the suspension injection are well described in the literature (Ref 64-66), and will not be elaborated here.

In parallel, it is noted that solution precursor has also been utilized for the deposition of functional coatings, e.g., protective manganese cobalt spinel coatings in SOFC interconnectors and ZrO₂-Al₂O₃ composite coatings, in a similar HVOF setup, and denser coatings were generally obtained (Ref 35, 67). In the case of dense ZrO₂-Al₂O₃ coatings, the concept of using HVOF process for solution spraying was successfully demonstrated. While in the spraying of the manganese cobalt spinel protective coatings, the effect of process parameters on the coating morphology was studied in details, and partially decomposed spinel crystalline phases were observed.

Some additional comments to fabricating SPPS coatings with HVOF torches are also provided here: (1) because the liquid injection occurs inside the combustion chamber of the gun, great care must be taken when injecting the feedstock as upon vaporization the volume of precursor expands and may cause the pressure to increase significantly; (2) pressure increase should be calculated along with the heat addition in the case of highly exothermic precursors, and (3) the higher pressure in the combustion chamber should be considered when choosing a precursor injector pressure, because it is the pressure drop that controls precursor flow rate. Good results can be achieved with the HVOF solution spraying process; however, lack of careful consideration of the above factors can potentially lead to undesirable development difficulties.

5. Future Directions

The SPPS process will advance one material system at a time basis because each chemical composition has its own challenges. Accordingly, the number of systems for which

the SPPS process can be used will continue to grow for the foreseeable future. Because of the deposition rate challenges, its most important role is likely to be rapid exploration of new compositions. The application where the SPPS process is currently regularly used is depositing thin thermographic phosphors. In this application, a thin specialized coating is needed and the lower deposition rate is not a serious drawback. The SPS process is now beginning to be used by gas turbine manufacturers to deposit thermal barrier coatings in spite of the deposition rate disadvantages it shares with the SPPS process. This application is driven by high performance requirement that is currently met by expensive electron beam physical vapor deposition processing (EBPVD). It is reasonable to expect the SPPS process to be used in this application as well since it is similar in most aspects. In fact, given the input materials costs and equivalent solution solids loading are somewhat more advantageous for the SPPS process compared to the SPS process and both are likely to have similar standoff distance limitations, there is no obvious reason that the SPPS process cannot compete with the SPS process in this developing application. There are two possible avenues to expand the applicability of the SPPS process by mitigating the low deposition rate disadvantage, which are learning how to use solvents with lower heat of vaporization, and better engineering the exploitation of exothermic chemical reactions. Advancements in the understanding of the APS process have been greatly assisted by diagnostic instruments that can measure particle velocity and temperature. Currently no similar instruments for the SPS and SPPS process are available because of the challenges associated with the small mean particle size in both processes. Development of such instruments would be highly desirable and further advance the success of these two processes.

6. Summary

Considerable progress has been in the process development, understanding, and applications for coatings made by the SPPS process. The prognosis for commercialization is increased because the SPS process, which uses the same liquid delivery system and suffers from deposition rate and standoff distance limitations, is being successfully applied.

The SPPS process along with the SPS process has the disadvantage of needing torch energy to evaporate the solvent or suspending liquid that leads to lower deposition rates compared to standard powder-based thermal spray. This disadvantage when using water appears to be approximately a factor of 4 on energy to produce melted ceramics at a given deposition rate. This of course can vary greatly depending on deposition efficiency. There are potential beneficial effects of lower energy of vaporization solvents or suspending liquids for SPS process, while taking advantage of exothermic chemical reactions is a natural feature of only the SPPS process. Recommendations have been provided for methods to prescreen

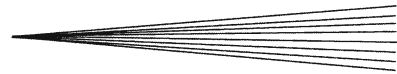
candidate precursors for use in the SPPS process, which save time and cost compared to just finding the performance by multiple spray trials.

Examples are shown that advantages of the unique features of the SPPS process are applicable to specific applications. These include (1) the production of stress-relieving cracks by pyrolysis shrinkage useful for thermal barrier coatings that mitigate the stresses due to thermal expansion mismatch with the metal substrate which enables the use of desirable coating materials (e.g., YAG) with larger expansion mismatch with the substrate to be used; (2) a fivefold increase in in-plane fracture toughness of TBC based on finer splats that likely plays a role in good erosion performance of several SPPS TBCs; (3) a twofold reduction of thermal conductivity in YSZ thermal barrier coatings by layered porosity (IPBs) produced using the SPPS process; (4) the production of extended metastable solubility of alumina in YSZ coatings for enhanced contaminant (CMAS) resistance of TBCs; (5) the production of a two-phase alumina/zirconia coating with very fine phase domains, (6) the production of a dense TiO₂ coating that can be made bioactive by post-treatment; (7) the successful solution spray of functional coatings using an HVOF torch; (8) the production of structures useful in fuel cells; and (ix) the ability when using the SPPS process to rapidly explore new compositions important in the development of thermographic phosphor coatings, YAG, and alumina-doped zirconia TBCs.

The SPPS process like all other coating processes has advantages and disadvantages which makes it very useful in specific applications and less so in others. This review should be of help in distinguishing between the two cases.

References

1. L. Pawlowski, Suspension and Solution Thermal Spray Coatings, *Surf. Coat. Technol.*, 2009, **203**(19), p 2807-2829
2. P. Fauchais, A. Joulia, S. Goutier, C. Chazelas, M. Vardelle, A. Vardelle, and S. Rossignol, Suspension and Solution Plasma Spraying, *J. Phys. D: Appl. Phys.*, 2013, **46**(22), p 224015
3. E.H. Jordan, L. Xie, M. Gell, N.P. Padture, B. Cetegen, A. Ozturk, X. Ma, J. Roth, T.D. Xiao, and P.E. Bryant, Superior Thermal Barrier Coatings Using Solution Precursor Plasma Spray, *J. Therm. Spray Technol.*, 2004, **13**(1), p 57-65
4. M. Gell, E.H. Jordan, M. Telcholz, B.M. Cetegen, N.P. Padture, L. Xie, D. Chen, X. Ma, and J. Roth, Thermal Barrier Coatings Made by the Solution Precursor Plasma Spray Process, *J. Therm. Spray Technol.*, 2008, **17**(1), p 124-135
5. A. Killinger, R. Gadow, G. Mauer, A. Guignard, R. Vassen, and D. Stöver, Review of New Developments in Suspension and Solution Precursor Thermal Spray Processes, *J. Therm. Spray Technol.*, 2011, **20**(4), p 677-695
6. O. Tingaud, P. Bertrand, and G. Bertrand, Microstructure and Tribological Behavior of Suspension Plasma Sprayed Al₂O₃ and Al₂O₃-YSZ Composite Coatings, *Surf. Coat. Technol.*, 2010, **205**(4), p 1004-1008
7. S. Kirihara, Y. Itakura, and S. Tasaki, Development of Thermal Spraying and Coating Techniques by Using Thixotropic Slurries Including Metals and Ceramics, *J. Phys.: Conf. Ser.*, 2013, **419**, p 0122039
8. J. Karthikeyan, C.C. Berndt, S. Reddy, J.-Y. Wang, A.H. King, and H. Herman, Nanomaterial Deposition Formed by DC Plasma Spraying of Liquid Feedstocks, *J. Am. Ceram. Soc.*, 1998, **81**(1), p 121-128
9. N.P. Padture, K.W. Schlichting, T. Bhatia, A. Ozturk, B. Cetegen, E.H. Jordan, M. Gell, S. Jiang, T.D. Xiao, P.R. Strutt, E. Garcia, P. Miranzo, and M.I. Osendi, Towards Durable Thermal Barrier Coatings with Novel Microstructures Deposited by Solution-Precursor Plasma Spray, *Acta Mater.*, 2001, **49**(12), p 2251-2257
10. T. Bhatia, A. Ozturk, L. Xie, E.H. Jordan, M. Gell, X. Ma, and N.P. Padture, Mechanisms of Ceramic Coating Deposition in Solution-Precursor Plasma Spray, *J. Mater. Res.*, 2012, **17**(9), p 2363-2372
11. L. Xie, X. Ma, E.H. Jordan, N.P. Padture, D.T. Xiao, and M. Gell, Identification of Coating Deposition Mechanisms in the Solution-Precursor Plasma-Spray Process Using Model Spray Experiments, *Mater. Sci. Eng. A*, 2003, **362**(1), p 204-212
12. L. Xie, X. Ma, E.H. Jordan, N.P. Padture, T.D. Xiao, and M. Gell, Deposition of Thermal Barrier Coatings Using the Solution Precursor Plasma Spray Process, *J. Mater. Sci.*, 2004, **39**(5), p 1636-1639
13. M. Gell, L. Xie, X. Ma, E.H. Jordan, and N.P. Padture, Highly Durable Thermal Barrier Coatings Made by the Solution Precursor Plasma Spray Process, *Surf. Coat. Technol.*, 2004, **177**, p 97-102
14. L. Xie, X. Ma, A. Ozturk, E.H. Jordan, N.P. Padture, B.M. Cetegen, D.T. Xiao, and M. Gell, Processing Parameter Effects on Solution Precursor Plasma Spray Process Spray Patterns, *Surf. Coat. Technol.*, 2004, **183**(1), p 51-61
15. L. Xie, E.H. Jordan, N.P. Padture, and M. Gell, Phase and Microstructural Stability of Solution Precursor Plasma Sprayed Thermal Barrier Coatings, *Mater. Sci. Eng. A*, 2004, **381**(1), p 189-195
16. Y.G. Shan, Y.L. Wang, and T. Coyle, Analysis of Deposits Formation in Plasma Spraying with Liquid Precursors, *Appl. Therm. Eng.*, 2013, **51**(1-2), p 690-697
17. L. Xie, D. Chen, E.H. Jordan, A. Ozturk, F. Wu, X. Ma, B.M. Cetegen, and M. Gell, Formation of Vertical Cracks in Solution-Precursor Plasma-Sprayed Thermal Barrier Coatings, *Surf. Coat. Technol.*, 2006, **201**(3), p 1058-1064
18. A.D. Jadhav, N.P. Padture, F. Wu, E.H. Jordan, and M. Gell, Thick Ceramic Thermal Barrier Coatings with High Durability Deposited Using Solution Precursor Plasma Spray, *Mater. Sci. Eng. A*, 2005, **405**(1), p 313-320
19. Y. Wang and T.W. Coyle, Solution Precursor Plasma Spray of Nickel-Yttria Stabilized Zirconia Anodes for Solid Oxide Fuel Cell Application, *J. Therm. Spray Technol.*, 2007, **16**(5), p 898-904
20. C.K. Muoto, E.H. Jordan, M. Gell, and M. Aindow, Identification of Desirable Precursor Properties for Solution Precursor Plasma Spray, *J. Therm. Spray Technol.*, 2011, **20**(4), p 802
21. D. Chen, E.H. Jordan, M. Gell, and X. Ma, Dense TiO₂ Coating Using the Solution Precursor Plasma Spray Process, *J. Am. Ceram. Soc.*, 2008, **91**(3), p 865-872
22. A. Aygun, A.L. Vasiliev, N.P. Padture, and X. Ma, Novel Thermal Barrier Coatings that are Resistant to High-Temperature Attack by Glassy Deposits, *Acta Mater.*, 2007, **55**(20), p 6734-6745
23. A.D. Jadhav, N.P. Padture, E.H. Jordan, M. Gell, P. Miranzo, and E.R. Fuller, Jr., Low-Thermal-Conductivity Plasma-Sprayed Thermal Barrier Coatings with Engineered Microstructures, *Acta Mater.*, 2006, **54**(12), p 3343-3349
24. E.H. Jordan, C. Jiang, J. Roth, and M. Gell, Low Thermal Conductivity Yttria-Stabilized Zirconia Thermal Barrier Coatings Using the Solution Precursor Plasma Spray Process, *J. Therm. Spray Technol.*, 2014, **23**(5), p 849-859
25. S.Y. Semenov and B.M. Cetegen, Spectroscopic Temperature Measurements in Direct Current Arc Plasma Jets Used in Thermal Spray Processing of Materials, *J. Therm. Spray Technol.*, 2001, **10**(2), p 326-336
26. S. Basu and B.M. Cetegen, Modeling of Thermo-physical Processes in Liquid Ceramic Precursor Droplets Injected into a Plasma Jet, *Int. J. Heat Mass Transf.*, 2007, **50**(17), p 3278-3290
27. E.H. Jordan, M. Gell, C. Jiang, J. Wang, and B. Nair, High Temperature Thermal Barrier Coating Made by the Solution Precursor Plasma Spray Process, *ASME Turbo Expo 2014: Turbine Technical Conference and Exposition*, Dusseldorf, Germany, 2014



28. D. Chen, E.H. Jordan, and M. Gell, Thermal and Crystallization Behavior of Zirconia Precursor Used in the Solution Precursor Plasma Spray Process, *J. Mater. Sci.*, 2007, **42**(14), p 5576-5580
29. D. Chen, E.H. Jordan, M. Gell, and X. Ma, Dense Alumina-Zirconia Coatings Using the Solution Precursor Plasma Spray Process, *J. Am. Ceram. Soc.*, 2008, **91**(2), p 359-365
30. S. Basu, E.H. Jordan, and B.M. Cetegen, Fluid Mechanics and Heat Transfer of Liquid Precursor Droplets Injected into High-Temperature Plasmas, *J. Therm. Spray Technol.*, 2008, **17**(1), p 60-72
31. D. Chen, E.H. Jordan, and M. Gell, Effect of Solution Concentration on Splat Formation and Coating Microstructure Using the Solution Precursor Plasma Spray Process, *Surf. Coat. Technol.*, 2008, **202**(10), p 2132-2138
32. D. Chen, E.H. Jordan, M. Gell, and M. Wei, Apatite Formation on Alkaline-Treated Dense TiO₂ Coatings Deposited Using the Solution Precursor Plasma Spray Process, *Acta Biomater.*, 2004, **4**(3), p 553-559
33. D. Chen, E.H. Jordan, and M. Gell, Porous TiO₂ Coating Using the Solution Precursor Plasma Spray Process, *Surf. Coat. Technol.*, 2008, **202**(24), p 6113-6119
34. D. Chen, E.H. Jordan, M.W. Renfro, and M. Gell, Dy:YAG Phosphor Coating Using the Solution Precursor Plasma Spray Process, *J. Am. Ceram. Soc.*, 2009, **92**(1), p 271-286
35. D. Chen, E.H. Jordan, and M. Gell, Solution Precursor High-Velocity Oxy-Fuel Spray Ceramic Coatings, *J. Eur. Ceram. Soc.*, 2009, **29**(16), p 3349-3353
36. D. Chen, E.H. Jordan, and M. Gell, The Solution Precursor Plasma Coatings: Influence of Solvent Type, *Plasma Chem. Plasma Process.*, 2010, **30**(1), p 111-119
37. D. Chen, E.H. Jordan, M.W. Renfro, and M. Gell, Solution Precursor Plasma Spray Eu: Y₂O₃ Phosphor Coating, *Int. J. Appl. Ceram. Technol.*, 2012, **9**(3), p 636-641
38. C. Metcalfe, J. Kuhn, and O. Kesler, Characterization of Ni-YSZ Anodes for Solid Oxide Fuel Cells Fabricated by Suspension Plasma Spraying with Axial Feedstock Injection, *J. Power Sour.*, 2013, **243**, p 172-180
39. W.Z. Wang, T. Coyle, and D. Zhao, Preparation of Lanthanum zirconate Coatings by the Solution Precursor Plasma Spray, *J. Therm. Spray Technol.*, 2014, **23**(5), p 827-832
40. Y. Wang and T.W. Coyle, Solution Precursor Plasma Spray of Porous La_{1-x}Sr_xMnO₃ Perovskite Coatings for SOFC Cathode Application, *J. Fuel Cell Sci. Technol.*, 2010, **8**(2), p 021005
41. Y. Wang and T.W. Coyle, Optimization of Solution Precursor Plasma Spray Process by Statistical Design of Experiment, *J. Therm. Spray Technol.*, 2008, **17**(5), p 692-699
42. S.V. Joshi, G. Sivakumar, T. Raghuvver, and R.O. Dusane, Hybrid Plasma-Sprayed Thermal Barrier Coatings Using Powder and Solution Precursor Feedstock, *J. Therm. Spray Technol.*, 2014, **23**(4), p 616-624
43. G. Sivakumar, R.O. Dusane, and S.V. Joshi, A Novel Approach to Process Phase Pure Alpha-Al₂O₃ Coatings by Solution Precursor Plasma Spraying, *J. Eur. Ceram. Soc.*, 2013, **33**(13-14), p 2823-2829
44. N. Sanpo, J. Wang, A.S.M. Ang, and C.C. Berndt, Influence of the Different Organic Chelating Agents on the Topography, Physical Properties and Phase of SPPS-Deposited Spinel Ferrite Splats, *Appl. Surf. Sci.*, 2013, **284**, p 171-178
45. Y. Shan, T.W. Coyle, and J. Mostaghimi, 3D Modeling of Transport Phenomena and the Injection of the Solution Droplets in the Solution Precursor Plasma Spraying, *J. Therm. Spray Technol.*, 2007, **16**(5), p 736-743
46. Y. Shan, T.W. Coyle, and J. Mostaghimi, Modeling the Influence of Injection Modes on the Evolution of Solution Sprays in a Plasma Jet, *J. Therm. Spray Technol.*, 2010, **19**(1), p 248-254
47. C. Marchand, C. Chazelas, G. Mariaux, and A. Vardelle, Liquid Precursor Plasma Spraying: Modeling the Interactions Between the Transient Plasma Jet and the Droplets, *J. Therm. Spray Technol.*, 2007, **16**(5), p 705-712
48. Y. Shan, T.W. Coyle, and J. Mostaghimi, Numerical Simulation of Droplet Breakup and Collision in the Solution Precursor Plasma Spraying, *J. Therm. Spray Technol.*, 2007, **16**(5), p 698-704
49. A. Vardelle, C. Chazelas, C. Marchand, and G. Mariaux, Modeling Time-Dependent Phenomena in Plasma Spraying of Liquid Precursors, *Pure Appl. Chem.*, 2008, **80**(9), p 1981-1991
50. A. Ozturk and B.M. Cetegen, Modeling of Plasma Assisted Formation of Precipitates in Zirconium Containing Liquid Precursor Droplets, *Mater. Sci. Eng. A*, 2004, **384**(1), p 331-351
51. A. Ozturk and B.M. Cetegen, Modeling of Axially and Transversely Injected Precursor Droplets into a Plasma Environment, *Int. J. Heat Mass Transf.*, 2005, **48**(21), p 4367-4383
52. Y. Shan, Z.P. Wei, T.W. Coyle, and J. Mostaghimi, Numerical Investigation of the Influence of Injected Modes in the Solution Precursor Plasma Spraying, *Proceedings of the International Thermal Spray Conference*, Las Vegas, NV, 2009
53. D. Soysal and A. Ansar, A New Approach to Understand Liquid Injection into Atmospheric Plasma Jets, *Surf. Coat. Technol.*, 2013, **220**, p 187-190
54. C.K. Muoto, E.H. Jordan, M. Gell, and M. Aindow, Effects of Precursor Chemistry on the Structural Characteristics of Y₂O₃-MgO Nanocomposites Synthesized by a Combined Sol-Gel/Thermal Decomposition Route, *J. Am. Ceram. Soc.*, 2011, **94**(2), p 372-381
55. A. Ozturk, Diagnostics and Modeling of Ytria-Stabilized Zirconia Formation in Solution Precursor Plasma Spray Process, Storrs CT, PhD thesis, 2005
56. K. VanEvery, M.J. Krane, R.W. Trice, H. Wang, W. Porter, M. Besser, D. Sordelet, J. Ilavsky, and J. Almer, Column Formation in Suspension Plasma-Sprayed Coatings and Resultant Thermal Properties, *J. Therm. Spray Technol.*, 2011, **20**(4), p 817-828
57. A. Joulia, G. Bolelli, E. Gualtieri, L. Lusvardi, S. Valeri, M. Varelle, S. Rossignol, and A. Vardelle, Comparing the Deposition Mechanisms in Suspension Plasma Spray (SPS) and Solution Precursor Plasma Spray (SPPS) Deposition of Ytria-Stabilized Zirconia (YSZ), *J. Eur. Ceram. Soc.*, 2014, **34**(15), p 3925-3940
58. H.B. Guo, H. Murakami, and S. Kuroda, Effect of Hollow Spherical Powder Size Distribution on Porosity and Segmentation Cracks in Thermal Barrier Coatings, *J. Am. Ceram. Soc.*, 2006, **89**(12), p 3797-3804
59. F. Tarasi, M. Medraj, A. Dolatabadi, J. Oberste-Berghaus, and C. Moreau, Amorphous and Crystalline Phase Formation During Suspension Plasma Spraying of the Alumina-Zirconia Composite, *J. Eur. Ceram. Soc.*, 2011, **31**(15), p 2903-2913
60. J. Oberste-Berghaus, J.-G. Legoux, C. Moreau, F. Tarasi, and T. Chraska, Mechanical and Thermal Transport Properties of Suspension Thermal-Sprayed Alumina-Zirconia Composite Coatings, *J. Therm. Spray Technol.*, 2008, **17**(1), p 91-104
61. C.S. Giggins, N.P. Anderson, R.S. Mullin, L.A. Riendeau, and N.E. Ulion, EB-PVD Method for Applying Ceramic Coatings, U.S. Patent 5087477 A, 5 Feb 1990
62. D.M. Gray, Y.-C. Lau, C.A. Johnson, M.P. Borom, and W.A. Nelson, Thermal Barrier Coatings Having an Improved Columnar Microstructure, U.S. Patent 5830586, 3 Nov 1998
63. B.S. Senturk, H.F. Garces, A.L. Ortiz, G. Dwivedi, S. Sampath, and N.P. Padture, CMAS-Resistant Plasma Sprayed Thermal Barrier Coatings Based on Y₂O₃-Stabilized ZrO₂ with Al³⁺ and Ti⁴⁺ Solute Additions, *J. Therm. Spray Technol.*, 2014, **23**(4), p 708-715
64. F.-L. Toma, L.-M. Berger, C.C. Stahr, T. Naumann, and S. Langner, Microstructures and Functional Properties of Suspension-Sprayed Al₂O₃ and TiO₂ Coatings: An Overview, *J. Therm. Spray Technol.*, 2010, **19**(1-2), p 262-274
65. J. Rauch, N. Stiegler, A. Killinger, and R. Gadow, High Velocity Suspension Flame Spraying (HVSFS): Process Development and Industrial Applications, *Thermal Spray 2009: Expanding Thermal Spray Performance to New Markets and Applications*, Las Vegas NV, 2009
66. R. Hui, J. Oberste-Berghaus, C. Deces-Petit, W. Ou, S. Yick, J.-G. Legoux, and C. Moreau, High Performance Metal-Supported Solid Oxide Fuel Cells Fabricated by Thermal Spray, *J. Power Sour.*, 2009, **191**, p 371-376
67. J. Puranen, J. Laakso, M. Kylmalahti, and P. Vuoristo, Characterization of High-Velocity Solution Precursor Flame-Sprayed Manganese Cobalt Oxide Spinel Coatings for Metallic SOFC Interconnectors, *J. Therm. Spray Technol.*, 2013, **22**(5), p 622-630